BNL-107198-2014-IR

Beam Energy Scan a Case for the Chiral Magnetic Effect in Au-Au Collisions

R.S. Longacre[1]

[1]Brookhaven National Laboratory, Upton, NY 11973 USA

December 2014

Physics Department

Brookhaven National Laboratory

U.S. Department of Energy
DOE Office of Science

Notice: This manuscript has been co-authored by employees of Brookhaven Science Associates, LLC under Contract No. DE-AC02-98CH10886 with the U.S. Department of Energy. The publisher by accepting the manuscript for publication acknowledges that the United States Government retains a non-exclusive, paid-up, irrevocable, world-wide license to publish or reproduce the published form of this manuscript, or allow others to do so, for United States Government purposes.

This preprint is intended for publication in a journal or proceedings. Since changes may be made before publication, it may not be cited or reproduced without the author's permission.

DISCLAIMER

This report was prepared as an account of work sponsored by an agency of the United States Government. Neither the United States Government nor any agency thereof, nor any of their employees, nor any of their contractors, subcontractors, or their employees, makes any warranty, express or implied, or assumes any legal liability or responsibility for the accuracy, completeness, or any third party's use or the results of such use of any information, apparatus, product, or process disclosed, or represents that its use would not infringe privately owned rights. Reference herein to any specific commercial product, process, or service by trade name, trademark, manufacturer, or otherwise, does not necessarily constitute or imply its endorsement, recommendation, or favoring by the United States Government or any agency thereof or its contractors or subcontractors. The views and opinions of authors expressed herein do not necessarily state or reflect those of the United States Government or any agency thereof.

Beam Energy Scan a Case for the Chiral Magnetic Effect in Au-Au Collisions.

R.S. Longacre[a]

[a]Brookhaven National Laboratory, Upton, NY 11973, USA

Abstract

The Chiral Magnetic Effect (CME) is predicted for Au-Au collisions at RHIC. However many backgrounds can give signals that make the measurement hard to interpret. The STAR experiment has made measurements at different collisions energy ranging from $\sqrt{s_{NN}}$=7.7 GeV to 62.4 GeV. In the analysis that is presented we show that the CME turns on with energy and is not present in central collisions where the induced magnetic is small.

1 Introduction

Topological configurations should occur in the hot Quantum Chromodynamic (QCD) vacuum of the Quark-Gluon Plasma (QGP) which can be created in heavy ion collisions. These topological configurations form domains of local strong parity violation (P-odd domains) in the hot QCD matter through the so-called sphaleron transitions. The domains might be detected using the Chiral Magnetic Effect (CME)[1] where the strong external magnetic field(electrodynamic) at the early stage of a collision(non-central), through the sphaleron transitions which induces a charge separation along the direction of the magnetic field perpendicular to the reaction plane. Such an out of plane charge separation, however, varies its orientation from event to event, either parallel or anti-parallel to the magnetic field (sphaleron or antisphaleron). Also the magnetic field can be up or down with respect to the reaction plane depending if the ions pass in a clockwise or anti-clockwise manner. Any P-odd observable will vanish and only the variance of such observable may be detected.

The STAR collaboration[2] has published a measurement of charge particle azimuthal correlations consistent with CME expectations. In Ref.[3] and used by STAR the CME can be indirectly approached through a two-particle azimuthal correlation given by

$$\gamma = \langle cos(\phi_1+\phi_2-2\Psi_{RP})\rangle = \langle cos(\phi_1-\Psi_{RP})cos(\phi_2-\Psi_{RP})\rangle - \langle sin(\phi_1-\Psi_{RP})sin(\phi_2-\Psi_{RP})\rangle, \tag{1}$$

where Ψ_{RP}, ϕ_1, ϕ_2 denote the azimuthal angles of the reaction plane, produced particle 1, and produced particle 2. This two particle azimuthal correlation measures the difference between the in plane and out of plane projected azimuthal correlation. If we would rotate all events such that $\Psi_{RP} = 0.0$, then γ would become

$$\gamma = \langle cos(\phi_1+\phi_2)\rangle = \langle cos(\phi_1)cos(\phi_2)\rangle - \langle sin(\phi_1)sin(\phi_2)\rangle. \tag{2}$$

The CME predicts that $\gamma > 0$ for opposite sign-pairs and $\gamma < 0$ for same sign-pairs. There are other two particle azimuthal correlation effects that can depend on the reaction plane

driven by elliptic flow even though the underlying correlation may be independent of the reaction plane. These backgrounds are summarized in Ref.[4]. It was pointed in Ref.[4] that the ϕ difference correlation (δ) which is independent of the reaction plane gives a constraint on the CME and backgrounds.

$$\delta = \langle cos(\phi_1 - \phi_2)\rangle = \langle cos(\phi_1)cos(\phi_2)\rangle + \langle sin(\phi_1)sin(\phi_2)\rangle. \tag{3}$$

In Ref.[4] Transverse Momentum Conservation (TMC) is derived and demonstrated that if there is no other correlation in the data except elliptic flow TMC will give a negative $\langle cos(\phi_1 + \phi_2 - 2\Psi_{RP})\rangle$ (γ) which is v_2 smaller than $\langle cos(\phi_1 - \phi_2)\rangle$ (δ). δ is a negative number given by TMC and scales as 1/N (N is the number of particles). Also in Ref.[4] Local Charge Conservation (LCC) is another important background and the details of LCC is found in Ref.[5]. The authors of Ref.[5] point out that for same sign pairs LCC should give a small negative sign, while for opposite sign pairs LCC should give a large positive correlation. Using the same coupling effect to the reaction plane as TMC, one should expect $\langle cos(\phi_1 + \phi_2 - 2\Psi_{RP})_{+-}\rangle$ (γ) equal v_2 times $\langle cos(\phi_1 - \phi_2)_{+-}\rangle$ (δ) for the LCC.

Ref.[1] has pointed out that P-odd domains on the surface of the fireball omit same charge sign particles in the direction of the magnetic field. The particles that escape the surface would be of the same sign while the charge particles moving in the opposite direction would be of opposite sign. These particles would run into the fireball and be thermalized and loss their direction (quenched). This effect will be taken into account in the latter part of this report.

The paper is organized in the following manner:

Sec. 1 is the introduction to correlations. Sec. 2 presents the STAR[6] correlation data which will be used in the analysis. Sec. 3 separates the correlations up into reaction plane dependent and independent parts with a further separation into charge dependent and charge independent amplitudes. Sec. 4 introduce ratios of charge dependent to total amplitudes. Sec. 5 brings the idea of quenching into the reaction plane dependent analysis. Sec. 6 presents the summary and discussion.

2 γ and δ from the Beam Energy Scan at RHIC

In this analysis we use STAR[6] data coming from charged particles produced in Au-Au collisions at RHIC. 8M $\sqrt{s_{NN}}$= 62.4 GeV (2005), 100M at 39.0 GeV (2010), 46M at 27.0 GeV (2011), 20M at 19.6 GeV (2011), 10M at 11.5 GeV (2010) and 4M at 7.7 GeV (2010) were used. γ ($\langle cos(\phi_1 + \phi_2 - 2\Psi_{RP})\rangle$) and δ ($\langle cos(\phi_1 - \phi_2)\rangle$) were extracted for like and unlike sign charged pairs as a function of centrality. Figure 1 - 4 show scatter plots of the correlation data. We have plotted centrality vs log($\sqrt{s_{NN}}$). In the plots the label E is equal to $\sqrt{s_{NN}}$ and the most central collisions are at 10% while most peripheral are at 70%. The vertical scale is measured in units of 10^{-4}. Figure 5 show the average v_2 plotted in the same type of scatter plot. This v_2 is needed to extract the reaction plane dependent and independent correlations which we define in Sec. 3.

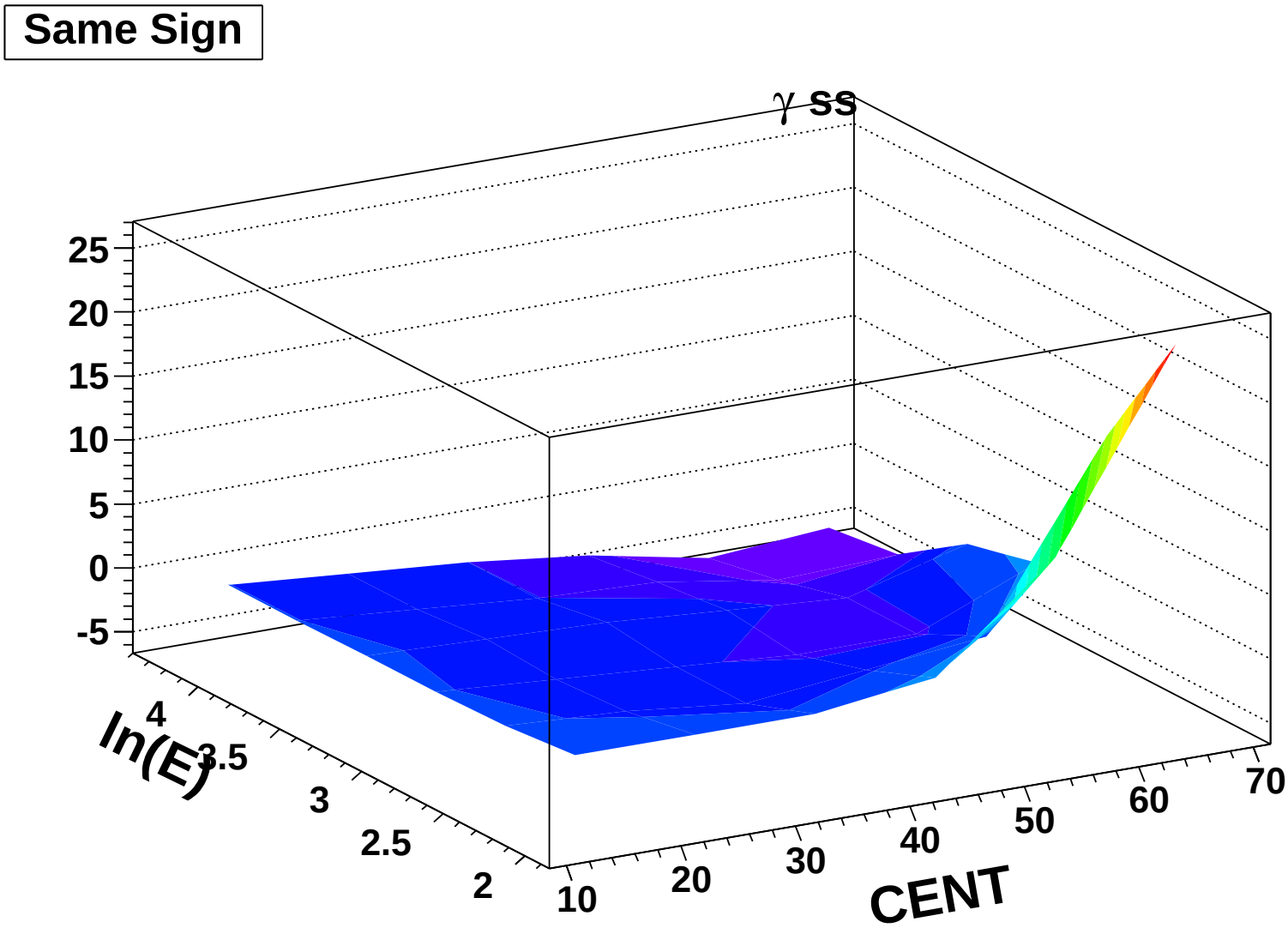

Figure 1: (Color) Scatter plot of the correlation(units of 10^{-4}) of same sign charge pairs $\langle cos(\phi_1 + \phi_2 - 2\Psi_{RP})\rangle$ (γ) calculated from Au-Au collisions with acceptance cuts of $0.15 < p_t < 2$ GeV/c and $|\eta| < 1.0$. The two axes are centrality vs beam energy. The beam energy is plotted as $\log(\sqrt{s_{NN}})$ with data from STAR[6] experiment at RHIC(see text). $\log(\sqrt{s_{NN}} = 64.4$ GeV$) = 4.1$ and $\log(\sqrt{s_{NN}} = 7.7$ GeV$) = 2.0$. Centrality ranges from most central collisions at 10%, while most peripheral at 70%.

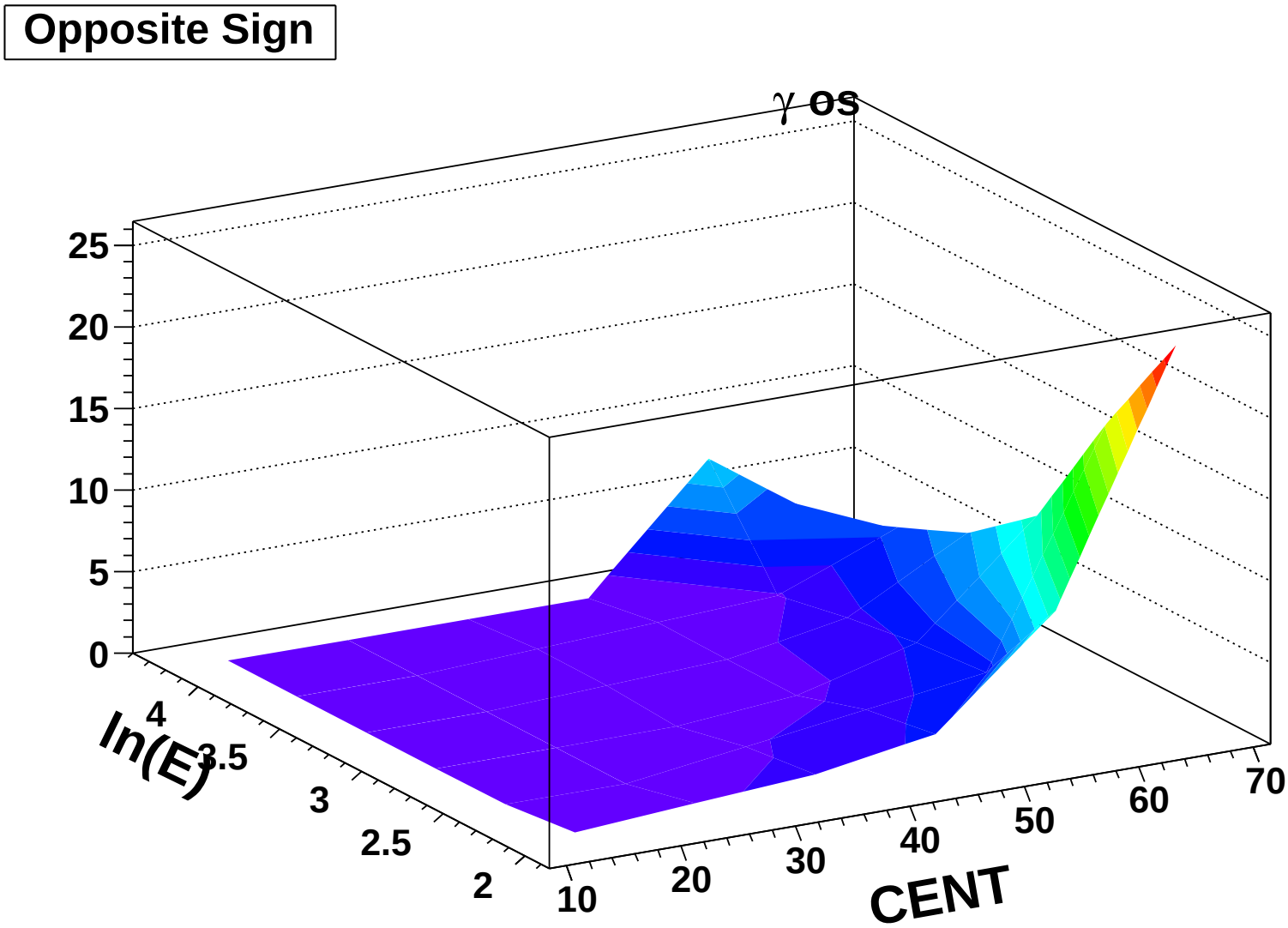

Figure 2: (Color) Scatter plot of the correlation(units of 10^{-4}) of opposite sign charge pairs $\langle cos(\phi_1 + \phi_2 - 2\Psi_{RP})\rangle$ (γ) calculated from Au-Au collisions with acceptance cuts of $0.15 < p_t < 2$ GeV/c and $|\eta| < 1.0$. The two axes are centrality vs beam energy. The beam energy is plotted as $\log(\sqrt{s_{NN}})$ with data from STAR[6] experiment at RHIC(see text). $\log(\sqrt{s_{NN}} = 64.4$ GeV$) = 4.1$ and $\log(\sqrt{s_{NN}} = 7.7$ GeV$) = 2.0$. Centrality ranges from most central collisions at 10%, while most peripheral at 70%.

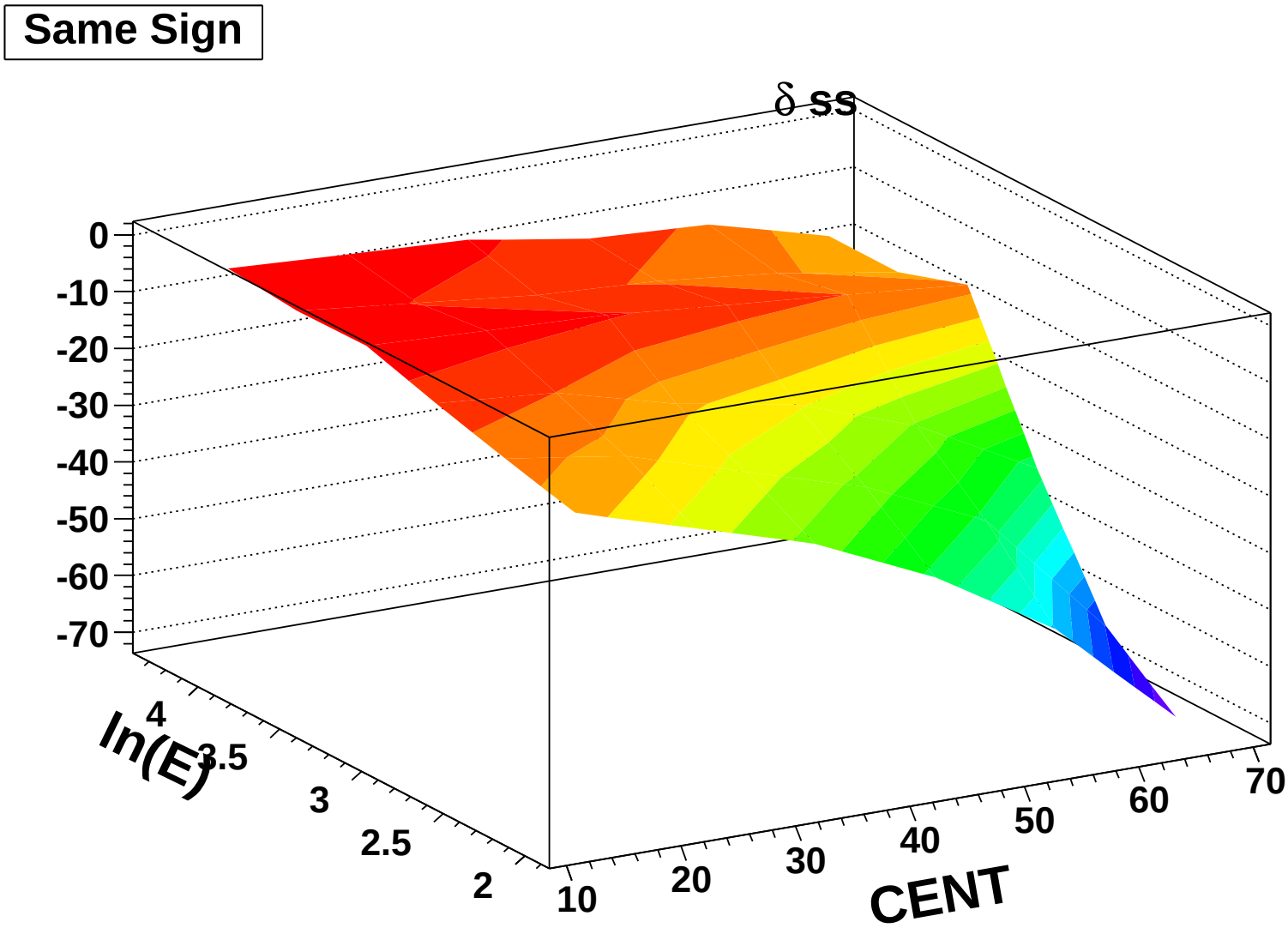

Figure 3: (Color) Scatter plot of the correlation(units of 10^{-4}) of same sign charge pairs $\langle cos(\phi_1 - \phi_2)\rangle$ (δ) calculated from Au-Au collisions with acceptance cuts of $0.15 < p_t < 2$ GeV/c and $|\eta| < 1.0$. The two axes are centrality vs beam energy. The beam energy is plotted as $\log(\sqrt{s_{NN}})$ with data from STAR[6] experiment at RHIC(see text). $\log(\sqrt{s_{NN}}$ = 64.4 GeV) = 4.1 and $\log(\sqrt{s_{NN}}$ = 7.7 GeV) = 2.0. Centrality ranges from most central collisions at 10%, while most peripheral at 70%.

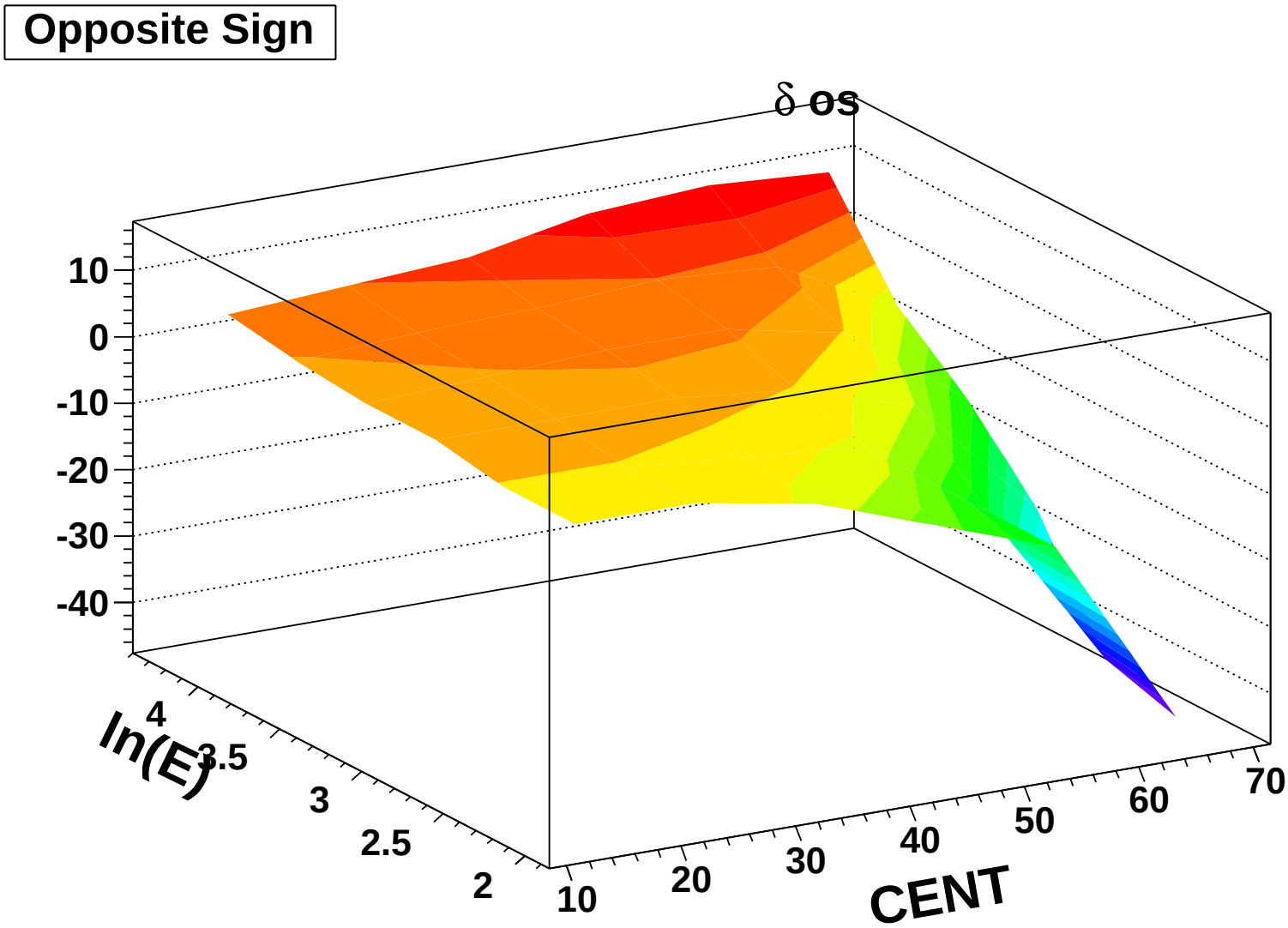

Figure 4: (Color) Scatter plot of the correlation(units of 10^{-4}) of opposite sign charge pairs $\langle cos(\phi_1 - \phi_2)\rangle$ (δ) calculated from Au-Au collisions with acceptance cuts of $0.15 < p_t < 2$ GeV/c and $|\eta| < 1.0$. The two axes are centrality vs beam energy. The beam energy is plotted as $\log(\sqrt{s_{NN}})$ with data from STAR[6] experiment at RHIC(see text). $\log(\sqrt{s_{NN}}$ = 64.4 GeV) = 4.1 and $\log(\sqrt{s_{NN}}$ = 7.7 GeV) = 2.0. Centrality ranges from most central collisions at 10%, while most peripheral at 70%.

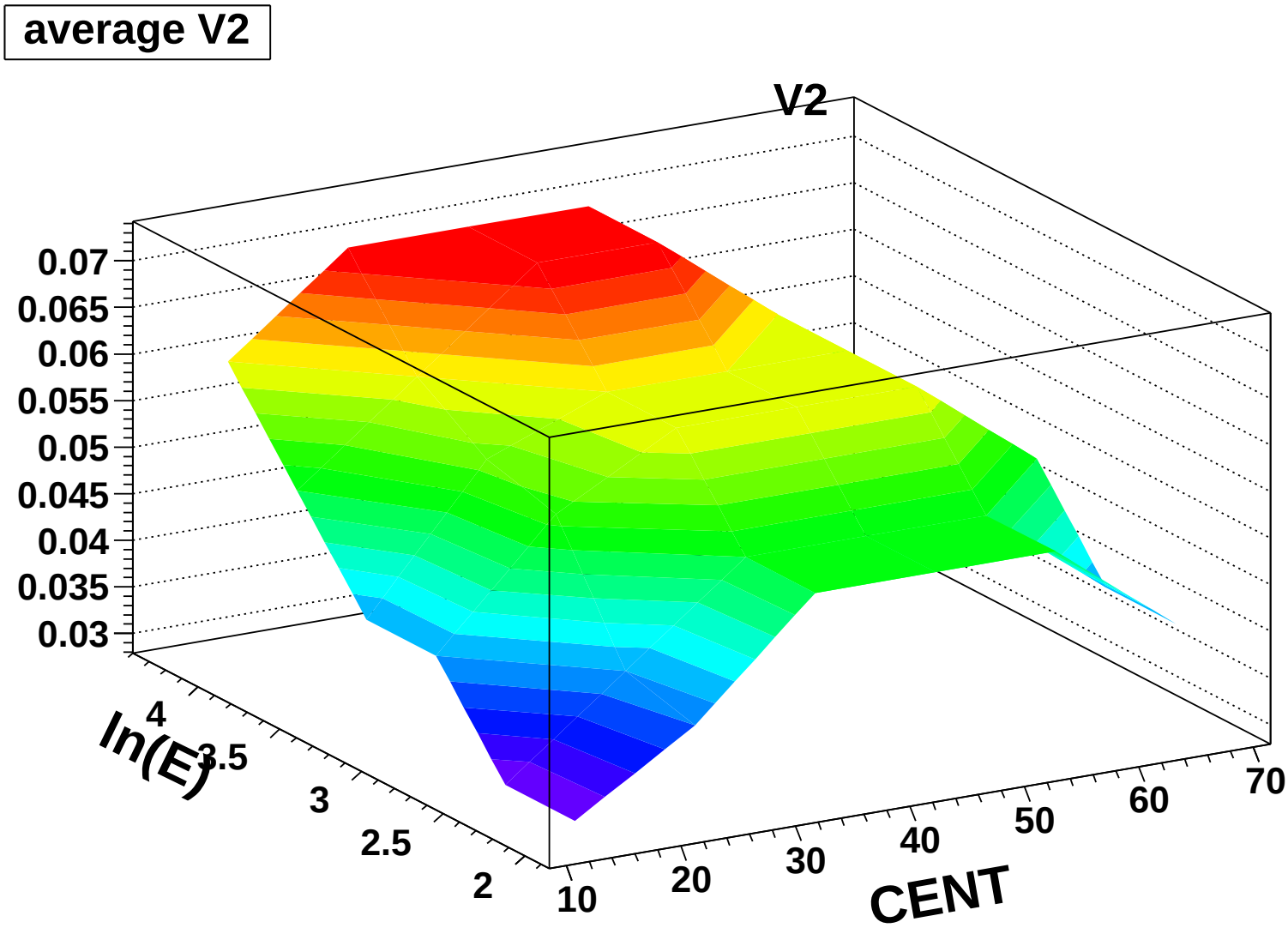

Figure 5: (Color) Scatter plot of the average v_2 calculated from Au-Au collisions with acceptance cuts of $0.15 < p_t < 2$ GeV/c and $|\eta| < 1.0$. The two axes are centrality vs beam energy. The beam energy is plotted as $\log(\sqrt{s_{NN}})$ with data from STAR[6] experiment at RHIC(see text). $\log(\sqrt{s_{NN}} = 64.4 \text{ GeV}) = 4.1$ and $\log(\sqrt{s_{NN}} = 7.7 \text{ GeV}) = 2.0$. Centrality ranges from most central collisions at 10%, while most peripheral at 70%.

3 Reaction Plane Dependent and Reaction Plane Independent Correlations

Using the γ and δ measurements we can define reaction plane dependent(H) and reaction plane independent(F) correlations. The definitions[6] from Ref.[7] are written as

$$\gamma = v_2 F - H, \tag{4}$$

and

$$\delta = F + H. \tag{5}$$

We can solve for H by using equations 4 and 5 obtaining

$$H = (v_2\delta - \gamma)/(1 + v_2). \tag{6}$$

Thus F is given by

$$F = \delta - H. \tag{7}$$

3.1 Charge Dependent and Charge Independent Amplitudes

The CME is a charge dependent amplitude. The CME amplitude has an opposite sign depending on whether we consider same sign charge pairs or opposite sign charge pairs. Also the CME is a reaction plane dependent amplitude acting on pairs which are moving along the B field perpendicular to the reaction plane. For this analysis we will assume that the CME is the only such effect at work when we isolate the reaction plane dependent(H) and charge dependent amplitude.

$$\text{HCME} = (H_{ss} - H_{os})/2, \tag{8}$$

where H_{ss} is the same sign charge pairs reaction plane dependent correlation and H_{os} is the opposite sign charge pairs reaction plane dependent correlation(see Figure 6). At low $\log(\sqrt{s_{NN}} = 7.7 \text{ GeV}) = 2.0$ HCME is very small, while at $\log(\sqrt{s_{NN}} = 64.4 \text{ GeV}) = 4.1$ HCME becomes large $\sim$.0003. The highest value of HCME $\sim$.0005 is an isolated point at top energies(see rotated plot Figure 7). At all energies the HCME is small for central collisions(note B field is small for central collisions).

We can define three other amplitudes HCI(reaction plane dependent amplitude with no charge dependence), FCD(reaction plane independent amplitude with a charge dependence) and FCI(reaction plane independent amplitude with no charge dependence).

$$\text{HCI} = (H_{ss} + H_{os})/2, \tag{9}$$

$$\text{FCD} = (F_{ss} - F_{os})/2, \tag{10}$$

and

$$\text{FCI} = (F_{ss} + F_{os})/2. \tag{11}$$

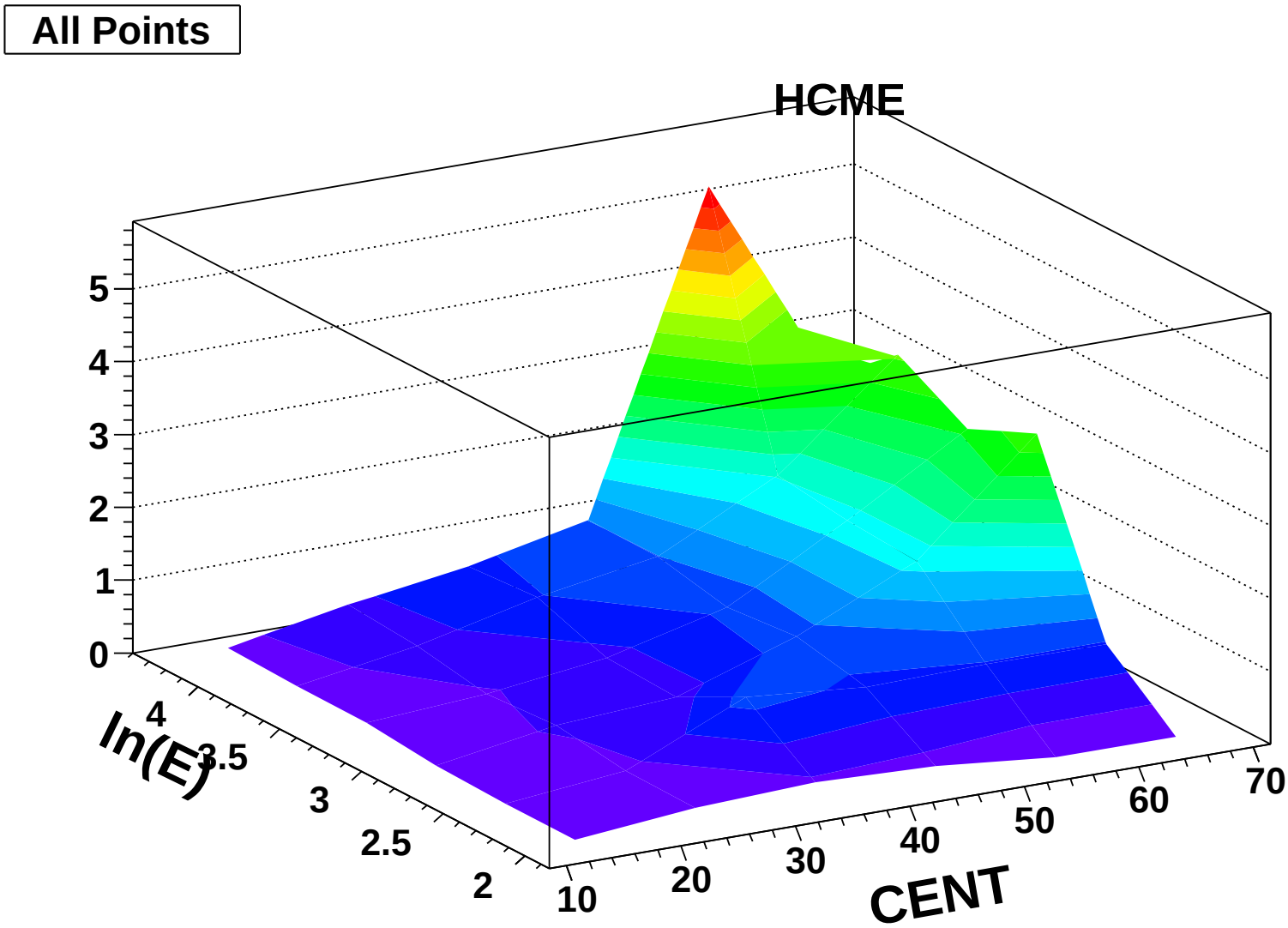

Figure 6: The HCME is assumed to dominate this charge sign dependent reaction plane dependent amplitude(units of 10^{-4}). The amplitude is calculated from Au-Au collisions with acceptance cuts of $0.15 < p_t < 2$ GeV/c and $|\eta| < 1.0$. The two axes are centrality vs beam energy. The beam energy is plotted as $\log(\sqrt{s_{NN}})$ with data from STAR[6] experiment at RHIC(see text). $\log(\sqrt{s_{NN}}) = 64.4$ GeV) $= 4.1$ and $\log(\sqrt{s_{NN}} = 7.7$ GeV) $= 2.0$. Centrality ranges from most central collisions at 10%, while most peripheral at 70%. HCME becomes large $\sim$.0003. The highest value of HCME $\sim$.0005 is an isolated at top energies(see rotated plot Figure 7). At all energies the HCME is small for central collisions(note B field is small for central collisions).

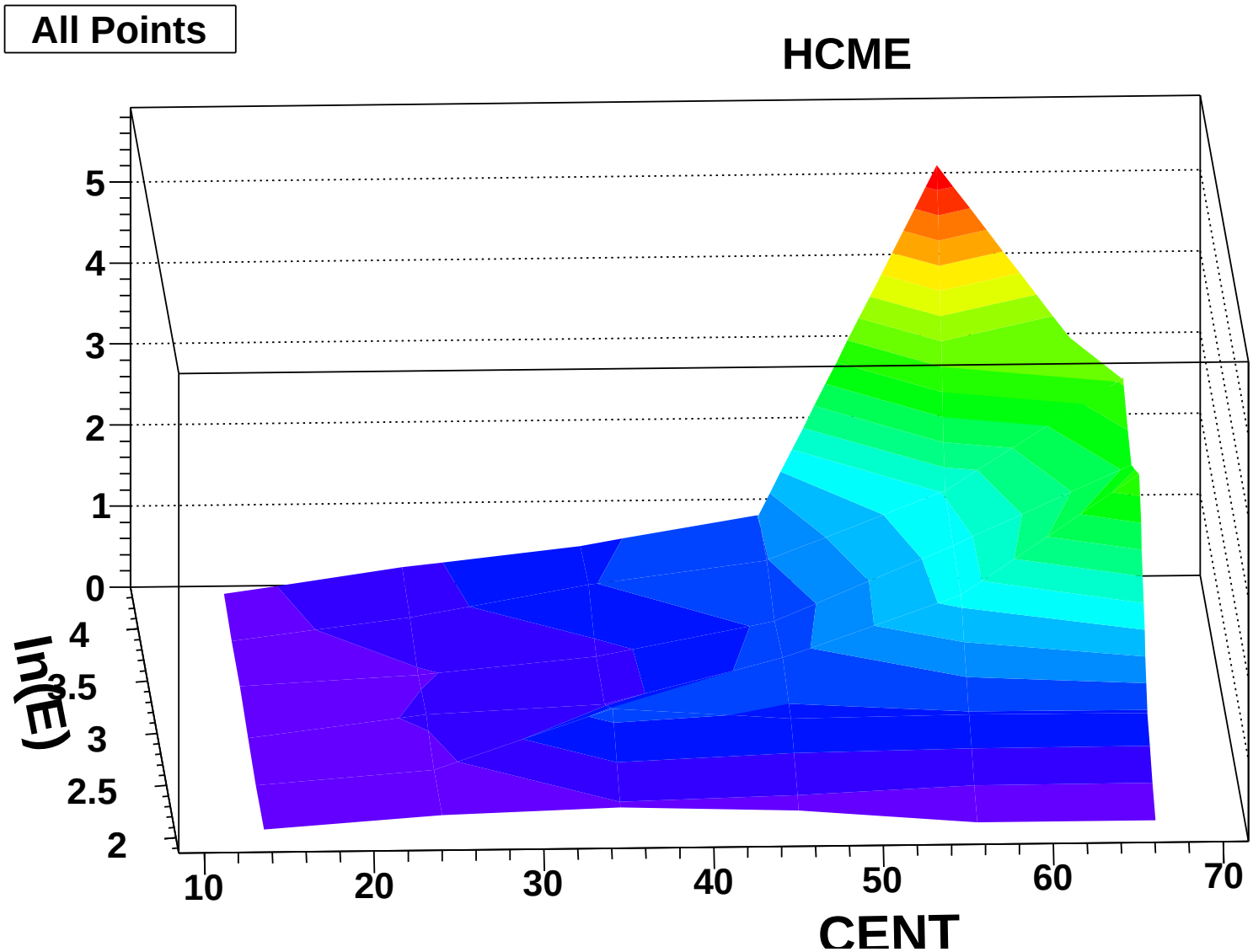

Figure 7: The HCME has been rotated so one can see that HCME $\sim$.0005 is an isolated value at top energies while sitting on a plateau of $\sim$.0003 in value. The amplitude(units of 10^{-4}) is calculated from Au-Au collisions with acceptance cuts of $0.15 < p_t < 2$ GeV/c and $|\eta| < 1.0$. The two axes are centrality vs beam energy. The beam energy is plotted as $\log(\sqrt{s_{NN}})$ with data from STAR[6] experiment at RHIC(see text). $\log(\sqrt{s_{NN}} = 64.4$ GeV) $= 4.1$ and $\log(\sqrt{s_{NN}} = 7.7$ GeV) $= 2.0$. Centrality ranges from most central collisions at 10%, while most peripheral at 70%

.

The HCI is dominate at low beam energy and most peripheral. HCI is a charge sign independent reaction plane dependent amplitude(units of 10^{-4}) as defined above. At lower beam energies and most peripheral the shower of charge particles from the Au-Au collision defines the reaction plane. This amplitude is negative which is driven by the back to back nature of the shower of particles due to momentum conservation. At the lowest beam energy the amplitude scales as 1/multiplicity(see Figure 8).

The FCD amplitude is a very complex two particle correlation where the same charge sign pair correlation has the opposite charge sign pair correlation subtracted from it. At the highest beam energies opposite sign particles are correlated with each other moving together and creating a positive sign(see Figure 4 and Ref.[8]). This positive correlation is stronger in the most peripheral collisions. The same charge sign correlation is negative arising from back to back correlation between like sign particles. The difference thus is an overall negative correlation which is strongest for the most peripheral collisions. When we plot the FCD in our usual scatter plot(see Figure 9) this high beam energy behavior is hidden by the more complicated action at lower beam energies. In Figure 10 we have rotated the plot so we can see this negative value at the most peripheral which decreases in absolute value as 1/multiplicity with centrality.

The FCI is dominate at low beam energy and most peripheral. FCI is a charge sign independent reaction plane independent amplitude(units of 10^{-4}) as defined above. At lower beam energies and most peripheral the shower of charge particles from the Au-Au collision have a back to back nature due to momentum conservation. The same charge sign pairs follow this basic behavior. Opposite charge sign pairs go against this behavior and cancel out this display of momentum conservation except for the most peripheral and lowest beam energy where momentum conservation is the strongest effect giving the largest negative amplitude of ∼-.0035 in this analysis(see Figure 11).

4 Ratio Charge Dependent Amplitudes to Total

For the higher beam energies the difference between the same charge sign pair correlation and the opposite charge sign pair correlation becomes vary large leading to dominance of charge dependent amplitudes. We can express this dominance by a ratio of the charge dependent to the square root of the sum of the squares of the charge dependent and the charge independent amplitudes. This ratio for the F or reaction plane independent amplitudes is given by

$$RF = FCD/\sqrt{FCD^2 + FCI^2}. \tag{12}$$

RF is shown in Figure 12 where for high beam energy this ratio is 1.0 dropping to 0.3 at the lowest energy and most peripheral.

The Chiral Magnetic Effect (HCME) is the dominate reaction plane and charge dependent amplitude for peripheral collision where there will be a magnetic field and high enough energy to have deconfined quarks. This ratio(RH) of the charge dependent to the square root of the

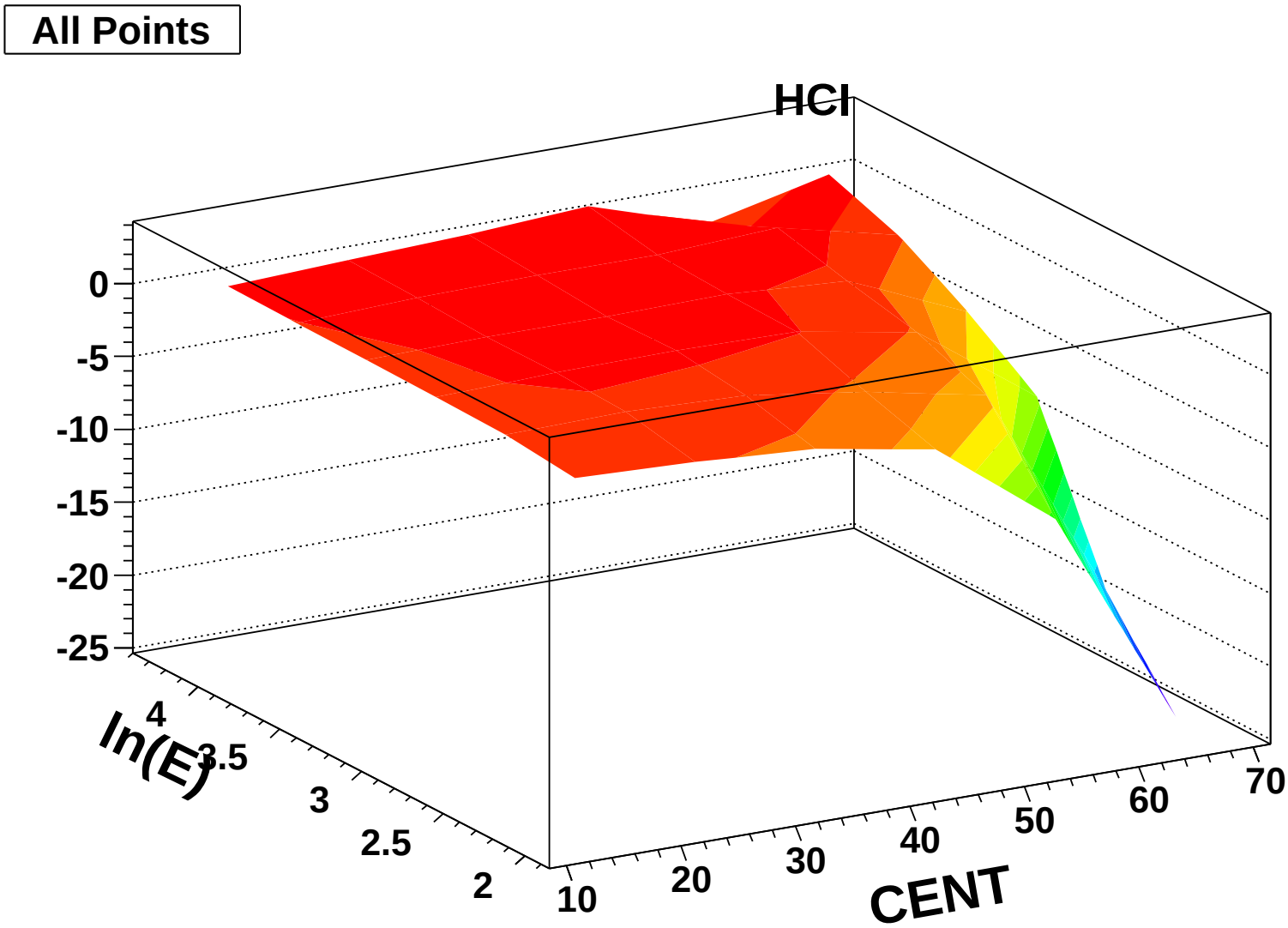

Figure 8: The HCI is dominate at low beam energy and most peripheral. HCI is a charge sign independent reaction plane dependent amplitude(units of 10^{-4}). The amplitude is calculated from Au-Au collisions with acceptance cuts of $0.15 < p_t < 2$ GeV/c and $|\eta| < 1.0$. The two axes are centrality vs beam energy. The beam energy is plotted as $\log(\sqrt{s_{NN}})$ with data from STAR[6] experiment at RHIC(see text). $\log(\sqrt{s_{NN}} = 64.4$ GeV$) = 4.1$ and $\log(\sqrt{s_{NN}} = 7.7$ GeV$) = 2.0$. Centrality ranges from most central collisions at 10%, while most peripheral at 70%. HCI has a large negative value ∼-.0025. This is a back to back pair correlation of momentum conservation. At the lowest beam energy the scaling is one of 1/multiplicity.

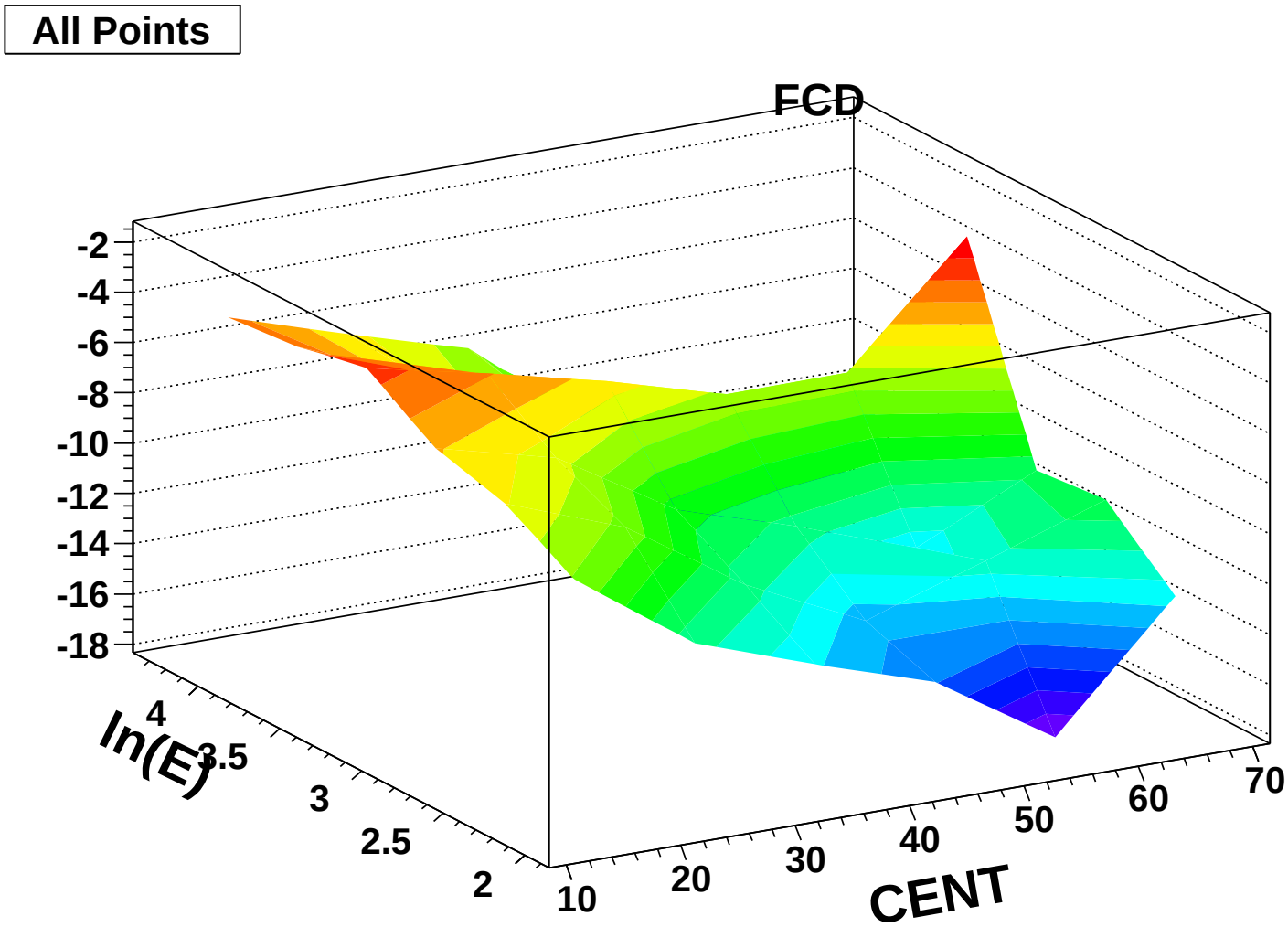

Figure 9: The FCD amplitude is a very complex two particle pair correlation where the same charge sign pair correlation has the opposite charge sign pair correlation subtracted from it. When we plot the FCD in our usual scatter plot the high beam energy behavior is hidden by the more complicated action at lower beam energies. In Figure 10 we have rotated the plot to so one can see the hidden behavior. FCD is a charge sign dependent reaction plane independent amplitude(units of 10^{-4}). The amplitude is calculated from Au-Au collisions with acceptance cuts of $0.15 < p_t < 2$ GeV/c and $|\eta| < 1.0$. The two axes are centrality vs beam energy. The beam energy is plotted as $\log(\sqrt{s_{NN}})$ with data from STAR[6] experiment at RHIC(see text). $\log(\sqrt{s_{NN}} = 64.4 \text{ GeV}) = 4.1$ and $\log(\sqrt{s_{NN}} = 7.7 \text{ GeV}) = 2.0$. Centrality ranges from most central collisions at 10%, while most peripheral at 70%. FCD has a large negative value ∼-.0018 for lowest beam energy and centrality of 55%.

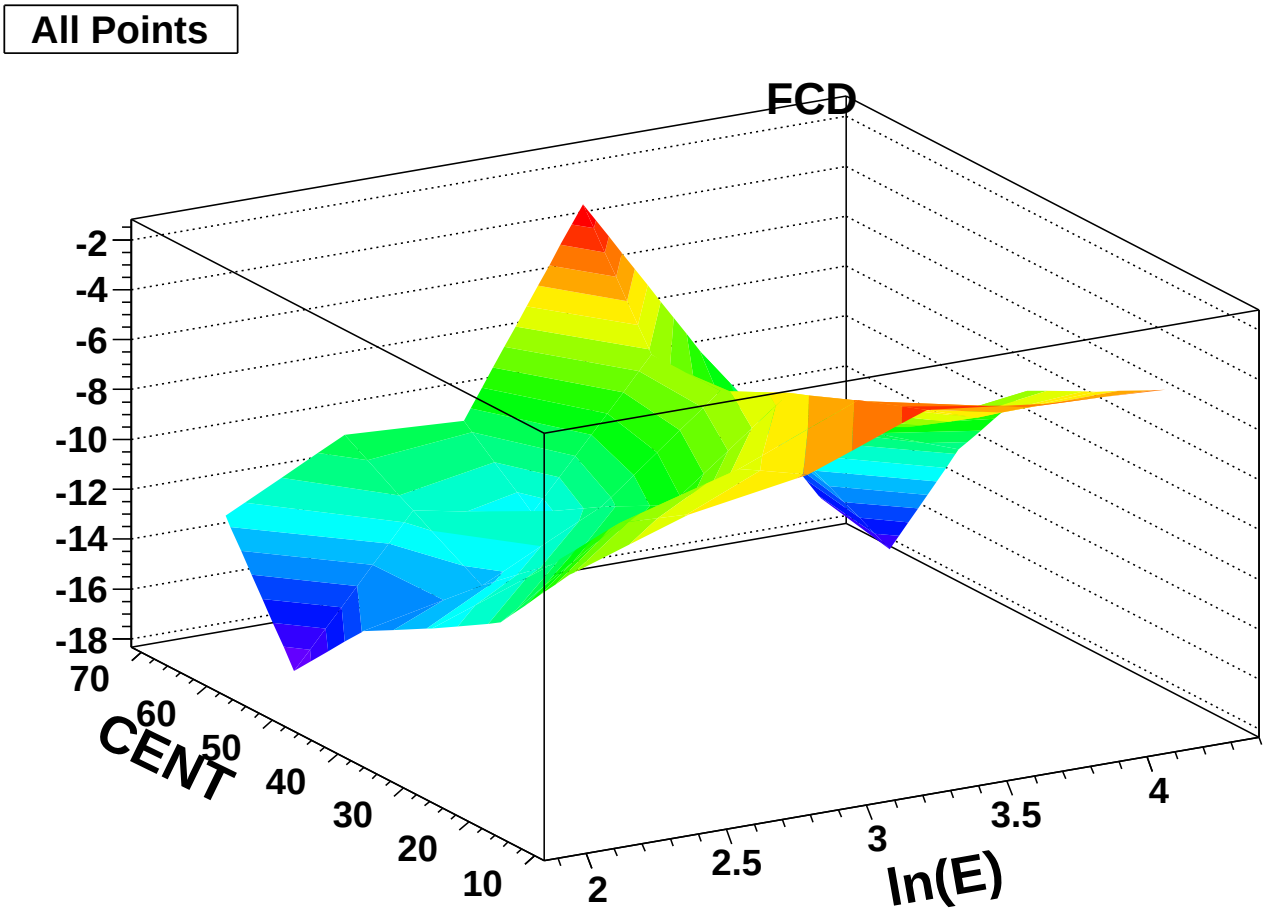

Figure 10: As part of the FCD amplitude at the highest beam energies the opposite sign particles pairs are correlated with each other moving together and creating a positive sign(see Figure 4 and Ref.[8]). This positive correlation is stronger in the most peripheral collisions but has a negative contribution to FCD. The same charge sign pair correlation is negative arising from back to back correlation between like sign particles and also makes the FCD more negative for peripheral collisions. Thus this overall negative correlation is strongest for the most peripheral collisions($\sim$-.0018). When we plot the FCD in our usual scatter plot(see Figure 9) this high beam energy behavior is hidden by the more complicated action at lower beam energies. In this figure we have rotated the plot so we can see this negative value at the most peripheral which decreases in absolute value as 1/multiplicity with centrality. The FCD is a charge sign dependent reaction plane independent amplitude(units of 10^{-4}). The amplitude is calculated from Au-Au collisions with acceptance cuts of $0.15 < p_t < 2$ GeV/c and $|\eta| < 1.0$. The two axes are centrality vs beam energy. The beam energy is plotted as $\log(\sqrt{s_{NN}})$ with data from STAR[6] experiment at RHIC(see text). $\log(\sqrt{s_{NN}} = 64.4$ GeV) $= 4.1$ and $\log(\sqrt{s_{NN}} = 7.7$ GeV) $= 2.0$. Centrality ranges from most central collisions at 10%, while most peripheral at 70%.

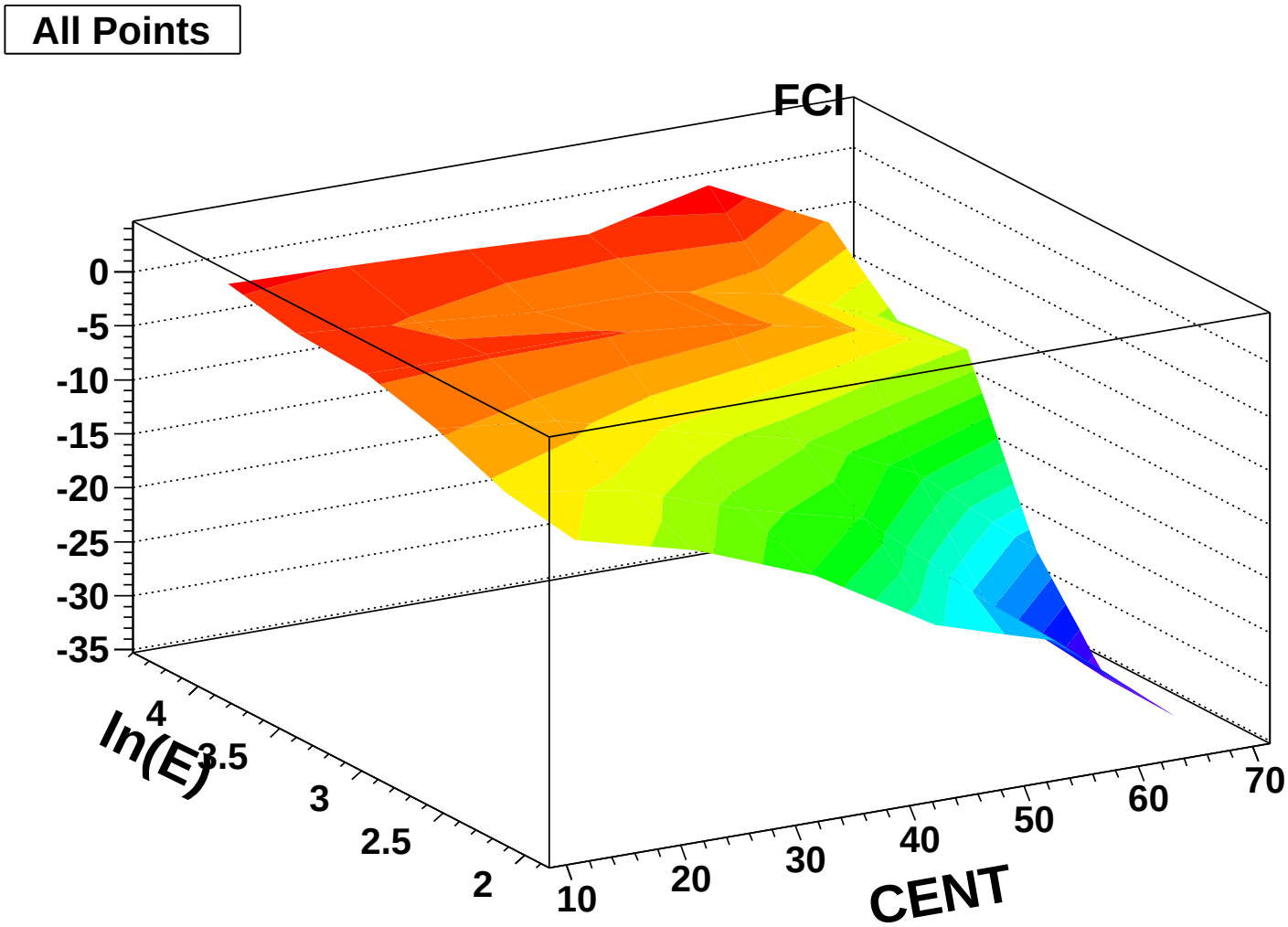

Figure 11: The FCI is dominate at low beam energy and most peripheral. FCI is a charge sign independent reaction plane independent amplitude(units of 10^{-4}). At lower beam energies and most peripheral the shower of charge particles from the Au-Au collision have a back to back nature due to momentum conservation. The same charge sign pairs follow this basic behavior. Opposite charge sign pairs go against this behavior and cancel out this display of momentum conservation except for the most peripheral and lowest beam energy where momentum conservation is the strongest effect giving ∼-.0035 the largest negative amplitude in this analysis. The amplitude is calculated from Au-Au collisions with acceptance cuts of $0.15 < p_t < 2$ GeV/c and $|\eta| < 1.0$. The two axes are centrality vs beam energy. The beam energy is plotted as $\log(\sqrt{s_{NN}})$ with data from STAR[6] experiment at RHIC(see text). $\log(\sqrt{s_{NN}} = 64.4 \text{ GeV}) = 4.1$ and $\log(\sqrt{s_{NN}} = 7.7 \text{ GeV}) = 2.0$. Centrality ranges from most central collisions at 10%, while most peripheral at 70%.

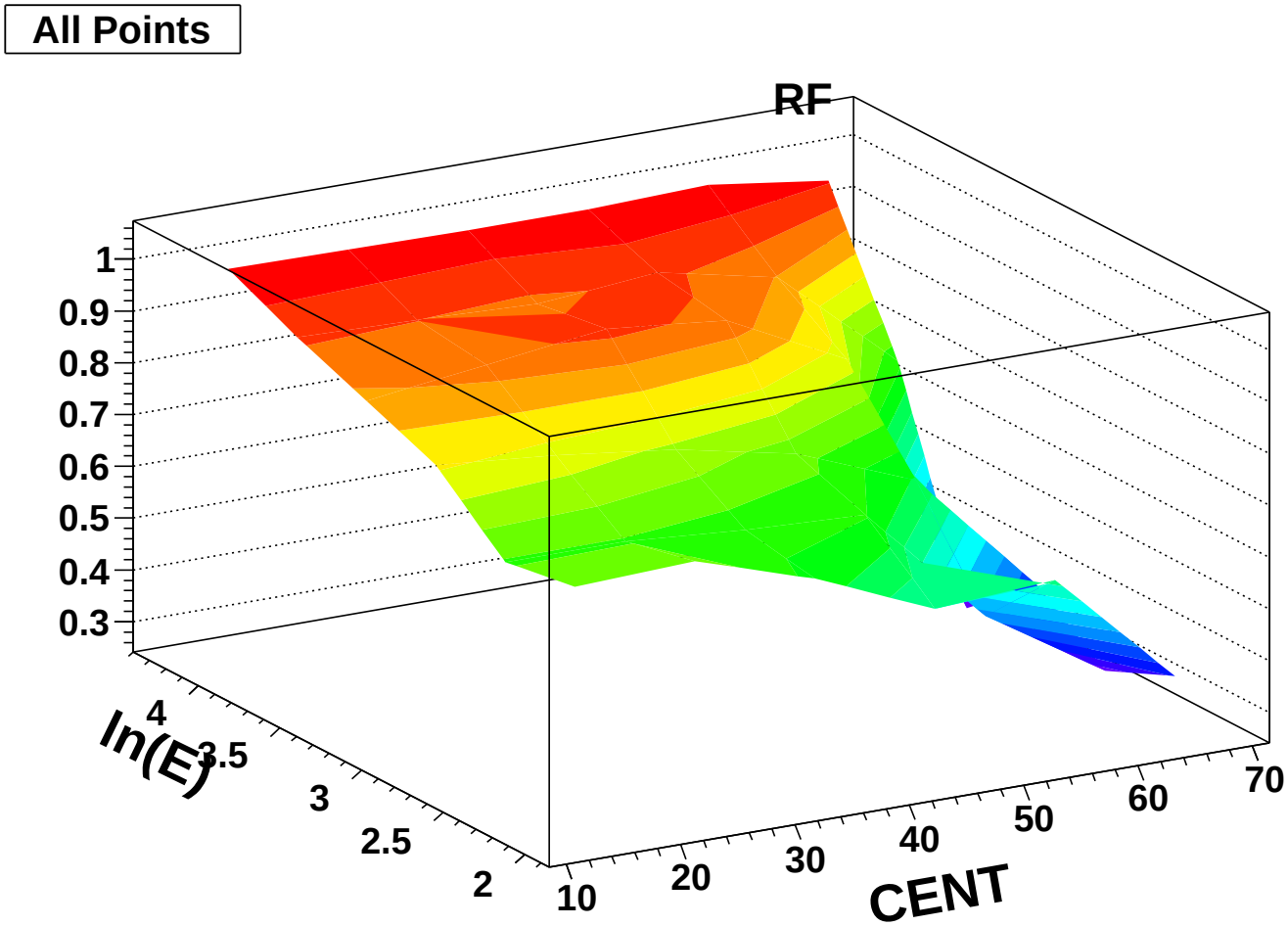

Figure 12: The ratio(RF) of the charge dependent to the square root of the sum of the squares of the charge dependent(FCD) and the charge independent amplitudes(FCI). This ratio RF for reaction plane independent amplitudes for the higher beam energies the difference between the same charge sign pair correlation and the opposite charge sign pair correlation becomes vary large leading to dominance of charge dependent amplitudes. The ratio is calculated from Au-Au collisions with acceptance cuts of $0.15 < p_t < 2$ GeV/c and $|\eta| < 1.0$. The two axes are centrality vs beam energy. The beam energy is plotted as $\log(\sqrt{s_{NN}})$ with data from STAR[6] experiment at RHIC(see text). $\log(\sqrt{s_{NN}} = 64.4 \text{ GeV}) = 4.1$ and $\log(\sqrt{s_{NN}} = 7.7 \text{ GeV}) = 2.0$. Centrality ranges from most central collisions at 10%, while most peripheral at 70%.

sum of the squares of the charge dependent and the charge independent amplitudes is

$$RH = HCME/\sqrt{HCME^2 + HCI^2}. \tag{13}$$

RH is shown in Figure 13 where the magnetic field is large and the energy is high enough for deconfined quarks the ratio is 1.0 dropping to zero at central events and low energies.

5 Quenching of the CME

Ref.[1] has pointed out that P-odd domains on the surface of the fireball omit same charge sign particles in the direction of the magnetic field. The particles that escape the surface would be of the same sign while the charge particles moving in the opposite direction would be of opposite sign. These particles would run into the fireball and be thermalized and loss their direction (quenched). This implies that H_{ss} would be unaffected by quenching, thus

$$H_{ss} = HCME + HCI. \tag{14}$$

If we would consider a quenching factor q such that when q equals 1 we have maximum quenching, H_{os} becomes

$$H_{os} = -(1-q)HCME + HCI. \tag{15}$$

Even though the CME is mainly in the same charge sign pairs the definition of the charge sign dependent reaction plane dependent amplitude remains the same. When there is quenching the relationship changes and the HCME becomes

$$(H_{ss} - H_{os})/2 = \left(\frac{2-q}{2}\right) HCME. \tag{16}$$

This causes in the maximum quenching case the HCME to be twice the value of the charge sign dependent reaction plane dependent amplitude(see Figure 14). the charge sign independent reaction plane dependent amplitude now picks up a component of the CME,

$$(H_{ss} + H_{os})/2 = \left(\frac{q}{2}\right) HCME + HCI. \tag{17}$$

However this has a very small effect on this amplitude(see Figure 15). Finally The ratio(RH) of the charge dependent to the square root of the sum of the squares of the charge dependent and the charge independent amplitudes is shown in Figure 16. We see that this ratio appears to have a nice gaussian shape which is consistent with there being quenching present in the reacting systems.

6 Summary and Discussion

We use the STAR[6] correlation data in an analysis that can separate the correlations up into reaction plane dependent and independent parts with a further separation into charge

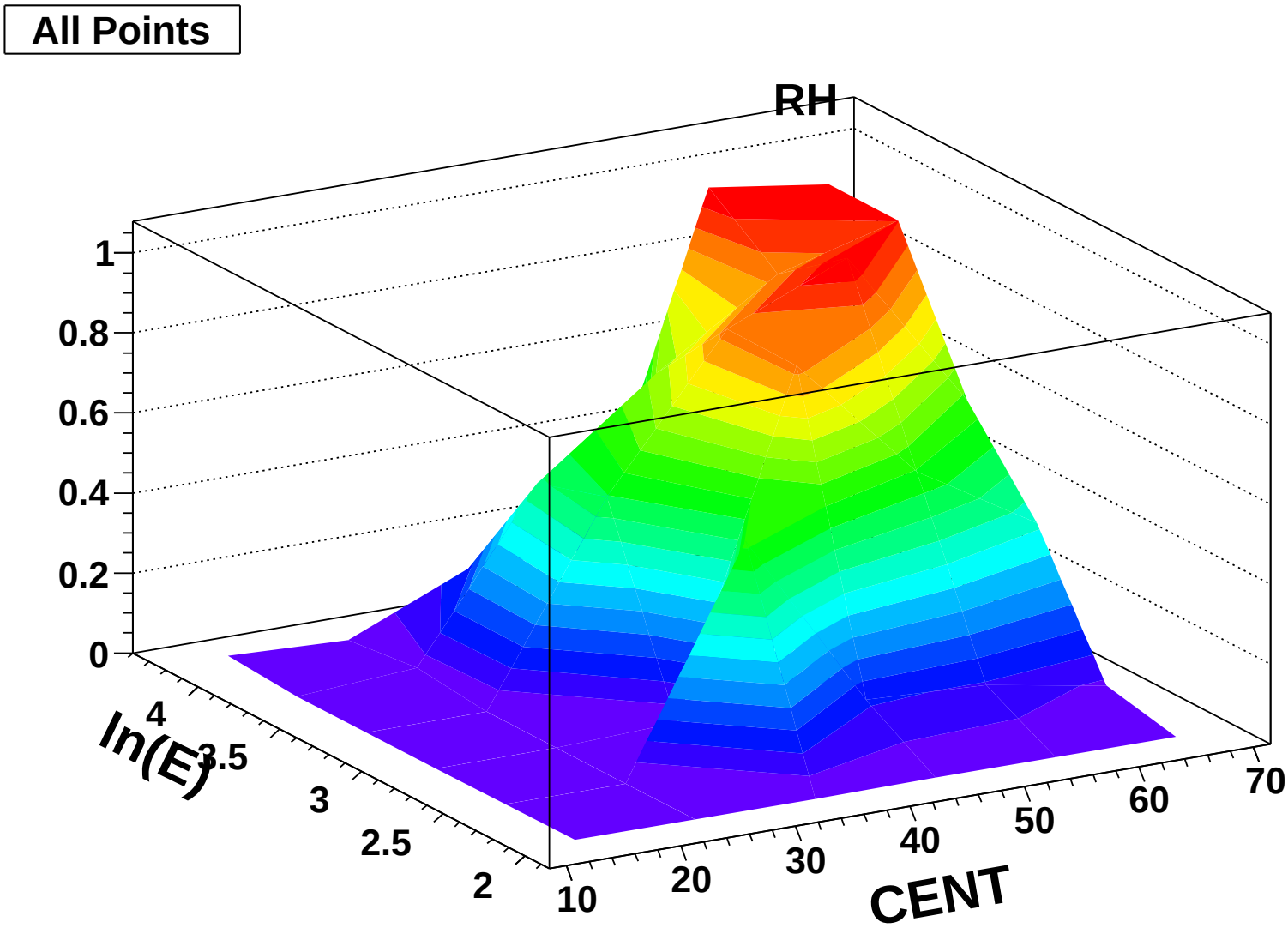

Figure 13: The ratio(RH) of the charge and reaction plane dependent to the square root of the sum of the squares of the charge dependent(HCME) and the charge independent amplitudes(HCI). This ratio RH for reaction plane dependent amplitudes for the higher beam energies(deconfined quarks) and peripheral collision (magnetic field) becomes vary large leading to dominance of charge dependent amplitudes. The ratio is calculated from Au-Au collisions with acceptance cuts of $0.15 < p_t < 2$ GeV/c and $|\eta| < 1.0$. The two axes are centrality vs beam energy. The beam energy is plotted as $\log(\sqrt{s_{NN}})$ with data from STAR[6] experiment at RHIC(see text). $\log(\sqrt{s_{NN}} = 64.4 \text{ GeV}) = 4.1$ and $\log(\sqrt{s_{NN}} = 7.7 \text{ GeV}) = 2.0$. Centrality ranges from most central collisions at 10%, while most peripheral at 70%.

dependent and charge independent amplitudes. This gives us a clean separation of the The Chiral Magnetic Effect into an amplitude HCME. This amplitude is isolated to top energies and peripheral collisions where the magnetic is field large and quarks are not confined. We also show that the idea of quenching is supported by the data best expressed by the ratio RH. This ratio(RH) of the charge dependent to the square root of the sum of the squares of the charge dependent and the charge independent amplitudes which we show in Figure 16 appears to have a nice gaussian shape. This is consistent with there being quenching present in the reacting systems.

7 Acknowledgments

This research was supported by the U.S. Department of Energy under Contract No. DE-AC02-98CH10886.

References

[1] D.E. Kharzeev, L.D. McLerran and H.J. Warringa, Nucl. Phys. A 803 (2008) 227.

[2] STAR Collaboration, B.I. Abelev *et al.*, Phys. Rev. Lett. 103 (2009) 251601, Phys. Rev. C 81 (2010) 054908.

[3] S.A. Voloshin, Phys. Rev. C 70 (2004) 057901.

[4] A. Bzdak, V. Koch and J. Liao, Phys. Rev. C 83 (2011) 014905.

[5] S. Schlichting and S. Pratt, arXiv:1005.5341[nucl-th].

[6] STAR Collaboration, L. Adamczyk *et al.*, Phys. Rev. Lett. 113 (2014) 052302.

[7] A. Bzdak, V. Koch and J. Liao, Lect. Notes Phys. 871 (2013) 503.

[8] J. Adams *et al.*, Phys. Lett B 634 (2006) 347, STAR Collaboration, M. Daugherity *et al.*, arXiv:0611.032[nucl-ex], STAR Collaboration, B.I. Abelev *et al.*, arXiv:0806.0513[nucl-ex].

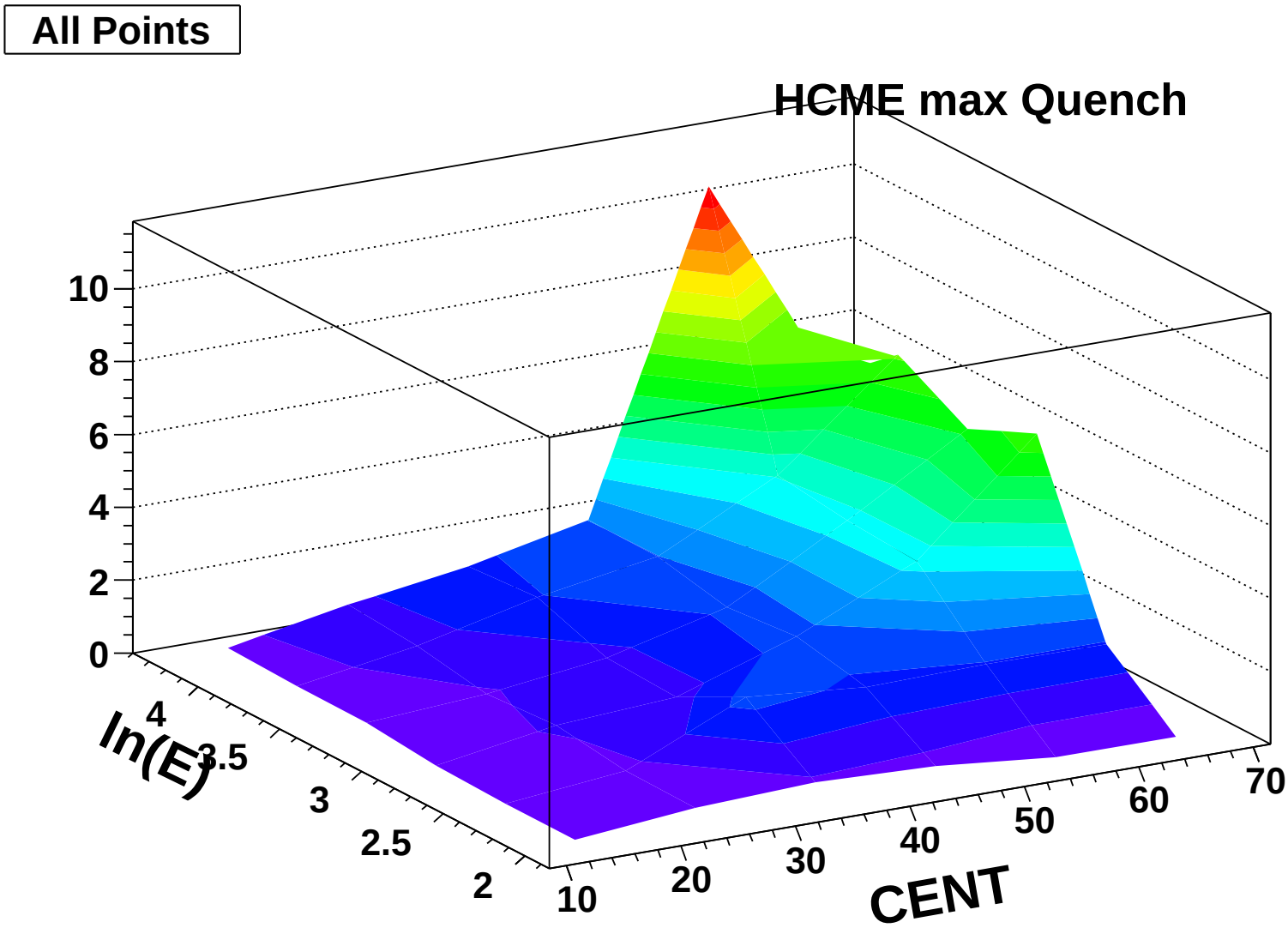

Figure 14: The HCME is assumed to dominate this charge sign dependent reaction plane dependent amplitude(units of 10^{-4}). Here we plot the HCME which would exist if there was maximum quenching. The amplitude is calculated from Au-Au collisions with acceptance cuts of $0.15 < p_t < 2$ GeV/c and $|\eta| < 1.0$. The two axes are centrality vs beam energy. The beam energy is plotted as $\log(\sqrt{s_{NN}})$ with data from STAR[6] experiment at RHIC(see text). $\log(\sqrt{s_{NN}}) = 64.4$ GeV) $= 4.1$ and $\log(\sqrt{s_{NN}} = 7.7$ GeV) $= 2.0$. Centrality ranges from most central collisions at 10%, while most peripheral at 70%. HCME becomes large $\sim$.0006. The highest value of HCME $\sim$.0010 is an isolated at top energies. At all energies central collisions the HCME is small(note B field is small at central collisions).

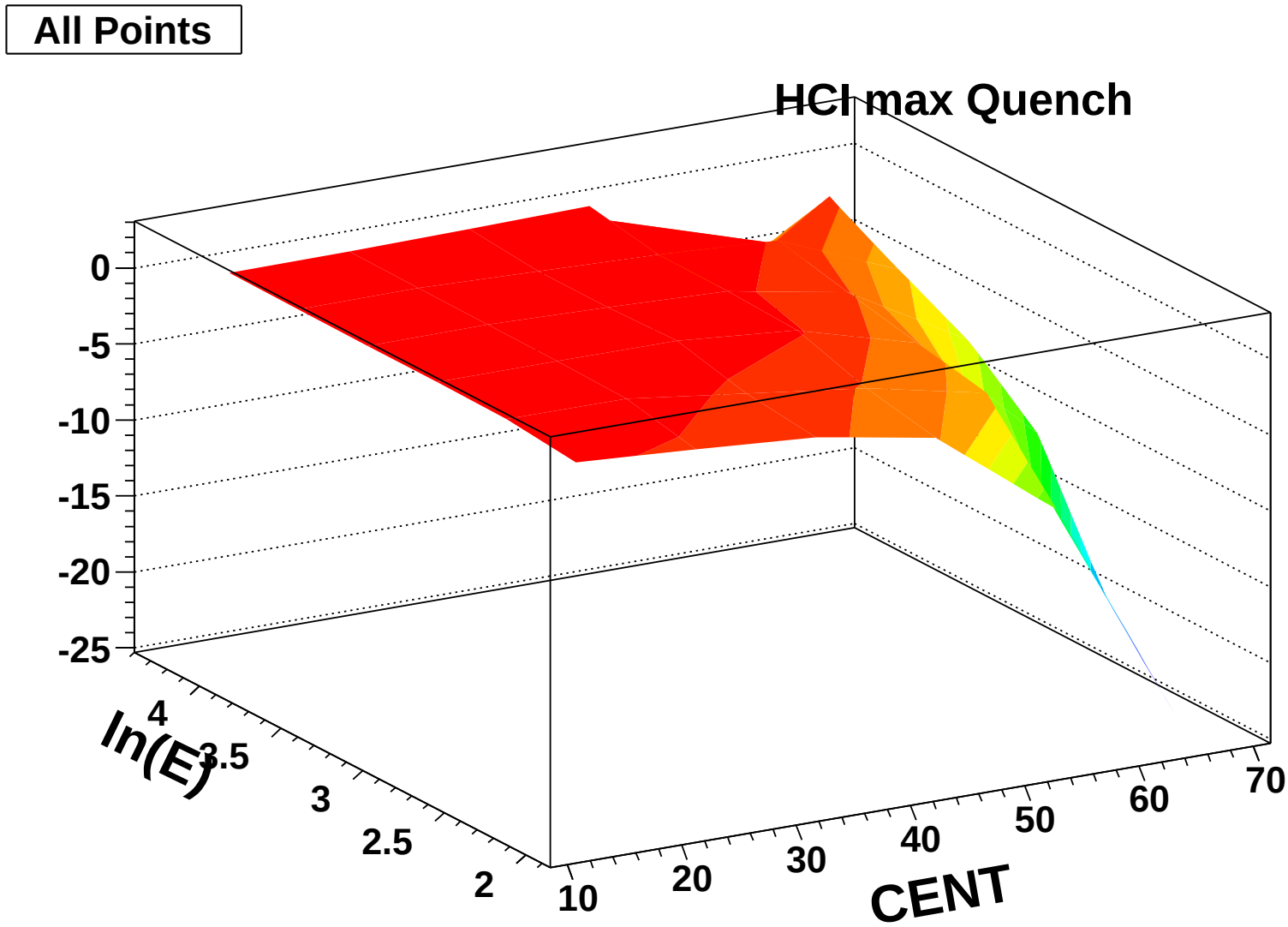

Figure 15: The HCI is dominate at low beam energy and most peripheral. Since this is the region where the CME is small quenching has little effect on this amplitude. HCI is a charge sign independent reaction plane dependent amplitude(units of 10^{-4}). The ratio is calculated from Au-Au collisions with acceptance cuts of $0.15 < p_t < 2$ GeV/c and $|\eta| < 1.0$. The two axes are centrality vs beam energy. The beam energy is plotted as $\log(\sqrt{s_{NN}})$ with data from STAR[6] experiment at RHIC(see text). $\log(\sqrt{s_{NN}} = 64.4 \text{ GeV}) = 4.1$ and $\log(\sqrt{s_{NN}} = 7.7 \text{ GeV}) = 2.0$. Centrality ranges from most central collisions at 10%, while most peripheral at 70%. HCI has a large negative value ∼-.0025. This is a back to back pair correlation of momentum conservation. At the lowest beam energy the scaling is one of 1/multiplicity.

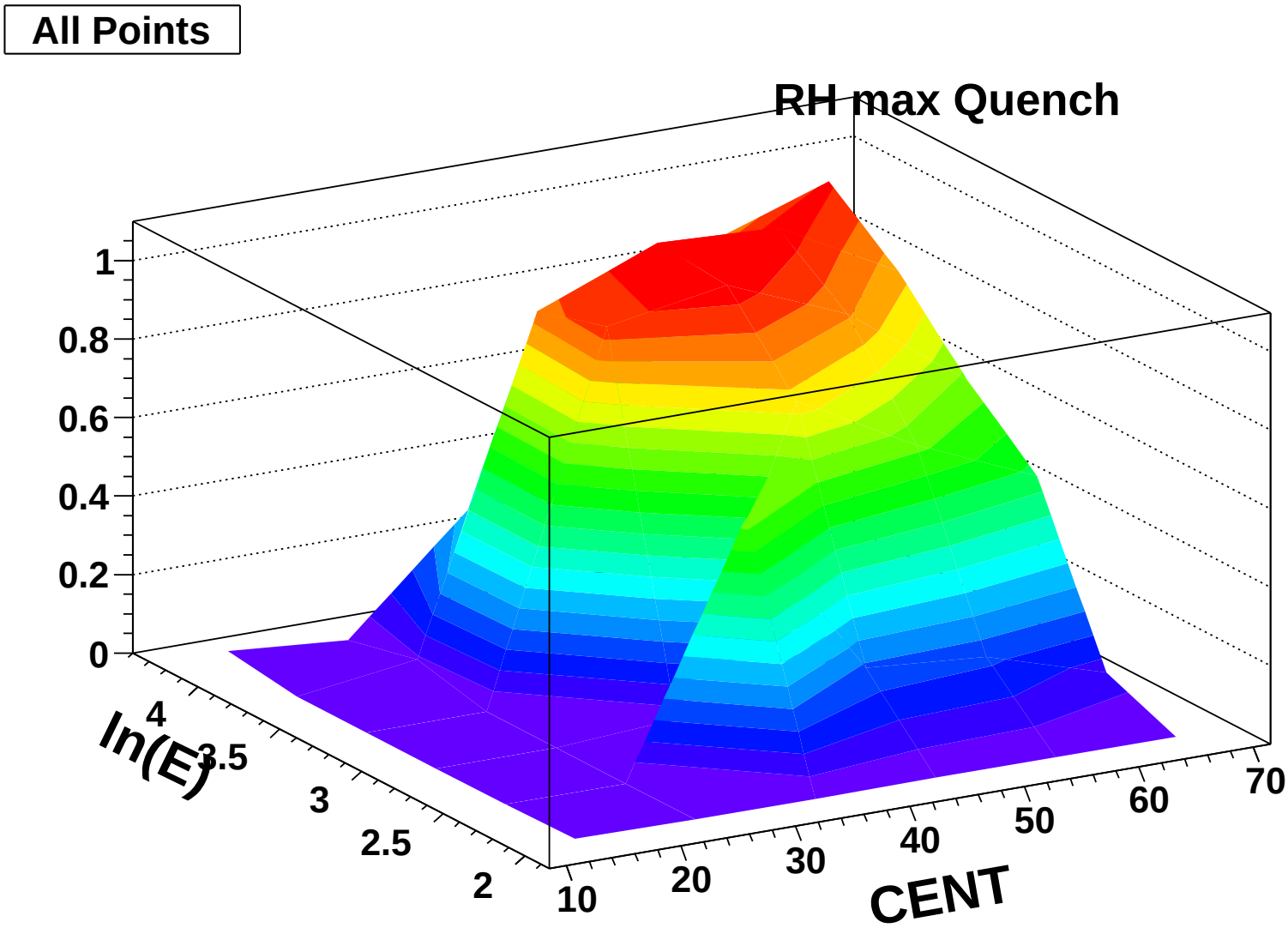

Figure 16: The ratio(RH) of the charge and reaction plane dependent to the square root of the sum of the squares of the charge dependent(HCME) and the charge independent amplitudes(HCI). This ratio RH for reaction plane dependent amplitudes for the higher beam energies(deconfined quarks) and peripheral collision (magnetic field) becomes vary large leading to dominance of charge dependent amplitudes. The amplitude is calculated from Au-Au collisions with acceptance cuts of $0.15 < p_t < 2$ GeV/c and $|\eta| < 1.0$. The two axes are centrality vs beam energy. The beam energy is plotted as $\log(\sqrt{s_{NN}})$ with data from STAR[6] experiment at RHIC(see text). $\log(\sqrt{s_{NN}} = 64.4 \text{ GeV}) = 4.1$ and $\log(\sqrt{s_{NN}} = 7.7 \text{ GeV}) = 2.0$. Centrality ranges from most central collisions at 10%, while most peripheral at 70%.